Check for updates

Efficient solvent-free mechanochemical synthesis of CALF-20 for carbon dioxide capture

Natchaya Phongsuk,[a] Chalarat Chaemchamrat,[a] Taya Ko Saothayanun, [iD][a] Nopphon Weeranoppanant [iD][b] and Sareeya Bureekaew [iD] *[a]

A solvent-free mechanochemical synthesis of CALF-20 is proposed, offering a rapid and cost-effective route by eliminating the solvent used and the purification process. With a record space–time yield of up to 88 000 kg m^{-3} d^{-1}, the mechano-synthesized CALF-20 exhibits a high CO_2 adsorption capacity, highlighting its potential for point-of-use carbon capture.

Carbon dioxide (CO_2), primarily emitted from fossil fuel combustion and industrial processes, is a key contributor to global climate change. To reduce its impact, various CO_2 capture technologies have been developed. Among them, adsorption has emerged as a promising alternative to traditional amine scrubbing due to its lower energy consumption and ease of regeneration. Porous materials, such as activated carbons,[1,2] zeolites,[3] and metal–organic frameworks (MOFs),[4] have been extensively examined for their potential as CO_2 adsorbents. Activated carbons are inexpensive but often suffer from low selectivity and require high pressure and temperature due to their irregular structure and broad pore size distribution.[5] Zeolites, with their polar adsorption sites, exhibit reduced performance in humid environments where water competes with CO_2 for adsorption sites. MOFs offer customizable pore structures and chemistry, making them promising materials for selective and efficient CO_2 capture. Calgary Framework 20 (CALF-20), introduced by Shimizu and colleagues in 2021, has shown exceptional stability, high capacity, and selectivity under realistic conditions, including flue gases at 100 °C with water vapor and acidic components.[6–8] CALF-20 is currently used by the Canadian company Svante in their advanced carbon capture technology.[9,10] Remarkably, just one gram of CALF-20, with a surface area of about 500 m^2, can selectively capture large amounts of CO_2 while requiring only a small amount of energy for regeneration.

Structurally, CALF-20 features a robust framework composed of zinc ions coordinated with 1,2,4-triazolate (Tz) and oxalate (Ox) ligands, forming $Zn_2(Tz)_2(Ox)$. CALF-20 was originally synthesized *via* a solvothermal method in methanol, using zinc oxalate and Tz as the metal and ligand precursors. While this represented a significant advancement in CALF-20 development, the process was energy- and time-intensive, requiring heating at 180 °C for 48 hours and a large volume of solvent. The high solvent-to-solid ratio (η = 5.69 μL mg^{-1}) was needed to overcome the poor solubility of zinc oxalate, yet the yield was only 70%.[6] To improve efficiency, alternative synthetic strategies have been explored. One approach uses microwave-assisted solvothermal synthesis, which reduces the reaction time to 4 hours and increases the yield to 97%, although it still requires elevated temperatures of 180 °C and high pressures.[11] Another approach involves substituting zinc oxalate with zinc acetate, which enables CALF-20 to precipitate in water/methanol mixtures within 30 minutes at room temperature, achieving a 93.3% yield.[12] While these approaches successfully reduce the synthesis temperature and reaction time, they still require substantial solvent use (η = 2–12 μL mg^{-1}, see Table S1), resulting in significant solvent waste. Recovering and recycling these solvents at scale remains challenging. Furthermore, products synthesized with high η values are often obtained as pastes or slurries, necessitating all five processing steps *i.e.*, dissolution, precipitation/crystallization, washing, separation, and drying to accomplish the synthesis, as illustrated in Fig. 1. These increase complexity, processing time and energy usage, ultimately reducing overall production efficiency.

The mechanochemical synthesis method offers an effective, green, and rapid synthetic tool for driving chemical reactions by applying mechanical force to facilitate mixing activation.[13] Owing to its simplicity and environmental

[a] *School of Energy Science and Engineering, Vidyasirimedhi Institute of Science and Technology, 555 Moo 1 Payupnai, Wangchan, Rayong 21210, Thailand. E-mail: sareeya.b@vistec.ac.th*

[b] *Department of Chemical Engineering, Faculty of Engineering, Chulalongkorn University, 254 Phayathai Road, Pathum Wan, Bangkok 10330, Thailand*
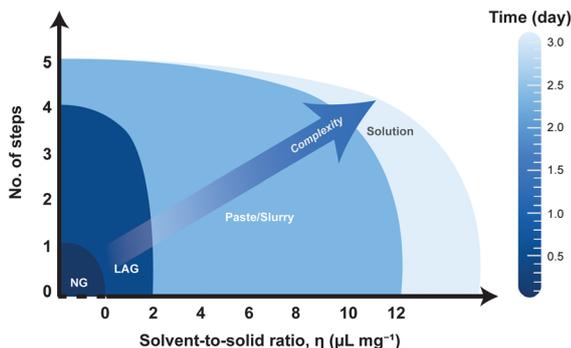
Fig. 1 Schematic illustration of the synthesis complexity of CALF-20 as a function of solvent-to-solid ratio (η). NG refers to neat grinding and LAG refers to liquid-assisted grinding.[16] The y-axis indicates the number of processing steps (no. of steps) required in the synthesis: (1) dissolution, (2) precipitation/crystallization, (3) washing, (4) separation and (5) drying. Color shading corresponds to the synthetic time, as shown in the scale bar. This visual highlights the relative complexity of each method. Additional details are provided in Table S1.

friendliness, mechanochemistry has attracted significant attention across various disciplines, including organic synthesis[14,15] and fabrication of advanced functional nanomaterials.[17–19] This technique has been successfully applied to the synthesis of several MOFs, such as ZIFs,[20,21] MOF-74,[22,23] MIL-100,[24] UiO-66,[25] HKUST-1,[26] and MOF-5.[27] To date, only a limited number of studies have explored the mechanochemical synthesis of CALF-20, particularly using liquid-assisted grinding (LAG) with η below 2 µL mg^{-1}. For example, in 2025, Raganati et al. reported the synthesis of CALF-20 within 1 hour using a mechanical milling method from zinc oxalate, Tz and a small quantity of methanol to perform LAG with η of 0.90 µL mg^{-1}.[28] However, reacting zinc oxalate with Tz at a stoichiometric ratio of 1 : 1.7 (with excess triazole) leads to the formation of oxalic acid as a by-product, thereby requiring a washing step.

In this study, we demonstrate a solvent-free mechanochemical approach for the synthesis of CALF-20, which eliminates the need for post-synthetic purification steps. Zinc acetate was selected as a metal precursor due to its chemical reactivity with Tz through acid–base interactions, facilitating the formation of the zinc-triazolate coordination network. Additionally, zinc acetate offers a cost-effective alternative to the conventionally used zinc oxalate. Alongside, Ox and Tz were employed as organic ligands in the synthesis. This substitution notably lowers material costs. Furthermore, as η decreases from solution-based synthesis ($\eta > 12$ µL mg^{-1}) to neat grinding (NG: $\eta = 0$ µL mg^{-1}), a substantial reduction in synthesis complexity is achieved. Energy consumption, reaction time and the number of processing steps are significantly reduced. In addition, the process does not generate solvent waste during either the synthesis or post-synthesis stages, thereby reducing environmental impact, operational costs, and energy requirements typically associated with solvent handling and drying. As shown in Fig. 1, NG not only eliminates solvent use but also minimizes

the overall synthetic steps, offering a more energy-efficient, sustainable, and scalable route for CALF-20 production and supporting its potential for commercialization.

The mechanochemical synthesis of CALF-20 was achieved through the direct grinding of zinc acetate, Ox, and Tz using mechanical force as illustrated in Fig. 2a. Initially, the ternary-component mixture was manually ground for a few minutes at room temperature without the addition of solvent. A characteristic vinegar-like odor of acetic acid is continually detected during the grinding, which may indicate the initial coordination between zinc acetate and Tz, leading to the formation of the porous coordination network known as CALF-20 (Fig. 2a). Importantly, this synthesis route does not require any purification steps, underscoring its operational simplicity and efficiency. The acetic acid by-product, which has a boiling point of approximately 118 °C, can be readily removed during the standard activation process typically employed prior to the use of CALF-20 in adsorption applications.

The phase formation and purity of the as-prepared solids were confirmed using a powder X-ray diffractometer (PXRD). Based on the flexible feature of CALF-20, the PXRD pattern depends on the guest molecule inside the structure. The PXRD pattern of the CALF-20 sample synthesized via the conventional solution-based method (conv CALF-20) closely resembles that reported by Wei et al., which corresponds to the PXRD pattern of CALF-20 before activation (Fig. 2b).[29] Upon activation at 180 °C for 3 hours to eliminate moisture, the PXRD pattern shifts to align with the simulated pattern of CALF-20 reported by Lin et al. (Fig. S1).[6] This consistency confirms the successful formation of the expected framework.

Similarly, the PXRD patterns of the ground solids agree well with the simulated pattern of CALF-20, confirming the possible formation of CALF-20 via a solvent-free
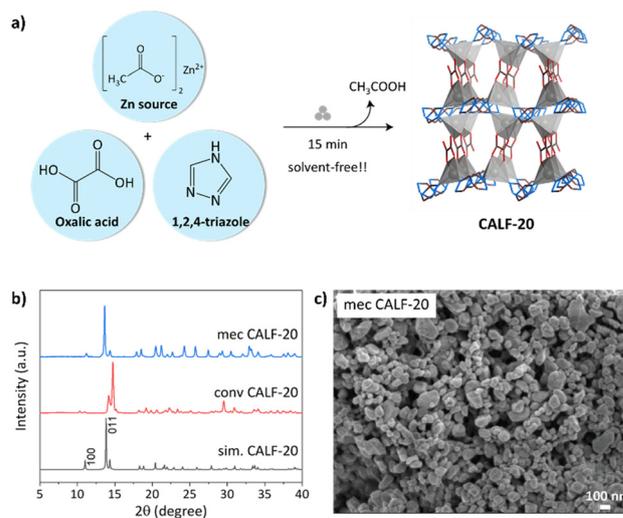

Fig. 2 (a) Chemical reaction and three-dimensional structure of CALF-20, (b) PXRD patterns of varying synthesis methods and (c) SEM image of mec CALF-20.

mechanochemical method without any purification process.[6] Notably, the characteristic reflections corresponding to the (100) and (011) planes are observed at 11.2° and 13.6°, respectively, indicating the α-phase structure of CALF-20.[30] The degree of similarity to the simulated pattern increases as the grinding exceeded 15 minutes (Fig. S2). Prolonging the grinding time to 45 minutes did not result in further significant changes, suggesting that 15 minutes is sufficient for complete phase formation. Interestingly, even a short grinding duration of 5 minutes yields CALF-20, although minor impurity peaks are observed at around $2\theta = 7.40°$ and 18.82°. These are likely attributable to intermediate species such as a Zn–triazole (Zn–Tz) complex or a Zn–oxalate (Zn–Ox) complex,[12] rather than the unreacted precursors (Fig. S3). The observation highlights the one-step mechanochemical approach, enabling the rapid formation of phase-pure CALF-20 within 15 minutes. The as-synthesized material, hereafter designated as mec CALF-20, was further evaluated for CO_2 adsorption performance to be compared with conventional CALF-20.

It is noted that the (011) reflection in the unwashed mec CALF-20 sample (Fig. S4) is slightly shifted toward a lower angle compared to the simulated CALF-20 pattern, due to the incorporation of acetic acid within the pores, in contrast to the solvothermal simulated counterparts that contain methanol. Consistent with the results observed for CALF-20 after the washing process, in which acetic acid is removed from the pores using water, the PXRD pattern clearly shows a shift in the (011) reflection compared to the unwashed sample (Fig. S4). Furthermore, the effect of precursor mixing order on CALF-20 formation was investigated. PXRD analysis revealed that CALF-20 forms successfully regardless of the mixing sequence in which the precursors are combined. As shown in Fig. S5, all samples exhibit PXRD patterns that are in good agreement with the simulated CALF-20 structure, confirming the versatility of the mechanochemical synthesis approach. The morphology of the synthesized particles was determined by scanning electron microscopy (SEM), as shown in Fig. 2c. The mec CALF-20 sample shows rounded nanoparticles with an average particle size of around 73.10 ± 19.90 nm. In contrast, the conv CALF-20 sample displays significantly larger particles with a broader and less uniform size distribution, as illustrated in Fig. S6. The smaller particle size in mec CALF-20 is likely due to the rapid, solvent-free synthesis achieved through 15 minutes of neat grinding. These nanoparticles, however, tend to aggregate (Fig. 2c), potentially requiring fluid-dynamic considerations in practical systems.[31]

The thermogravimetric (TG) profiles of all samples are shown in Fig. 3a. The initial weight losses of approximately 11% for conv CALF-20 and 6.5% for mec CALF-20 are observed below 113 °C, attributing to the evaporation of adsorbed moisture. In the case of mec CALF-20, an additional weight loss of around 9.4% occurs near 113 °C, which is attributed to the release of residual acetic acid retained within the pores of the framework. A major weight loss is
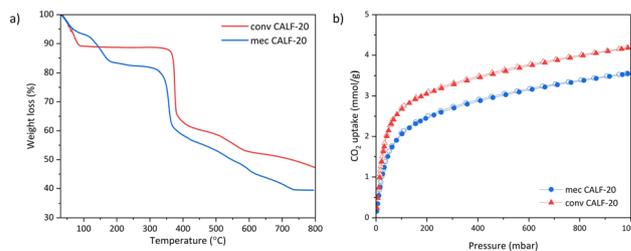

Fig. 3 (a) TG profiles and (b) CO_2 sorption isotherms obtained at 298 K for conv CALF-20 and mec CALF-20.

observed above 350 °C for both samples, indicating the thermal decomposition and structural collapse of the CALF-20 framework. It is worth noting that the acetic acid weight loss was found to be lower than the theoretical value (38% wt), due to partial evaporation during grinding and storage. This suggests that most of the acetic acid can be easily removed through spontaneous evaporation, while the remaining residue can be eliminated during the activation step, without the need for additional purification. The thermal stability of the activated mec CALF-20 is comparable to that of the conventional sample, as shown in Fig. S7. After thermal activation at 180 °C for 3 hours, the conditions typically used prior to CO_2 adsorption measurements, the TG profile of treated mec CALF-20 exhibits a single weight loss occurring below 113 °C, attributed solely to the removal of moisture. This indicates that the residual acetic acid is effectively removed upon activation.

In terms of synthesis efficiency, the yield of mec CALF-20, calculated based on the molar amount of zinc, exceeds 90% (based on dried weight), representing a significant improvement over the conventional method, which yields approximately 70%. Furthermore, the mechanochemical method achieves an outstanding space–time yield (STY) of 83 000 kg m^{-3} d^{-1}, calculated based on the volume of precursors used. This value is significantly higher than the typical STYs reported for other MOFs under optimized conditions, such as MOF-303, MIL-160, Al-fumarate, and even CALF-20, which generally range from 180 to 3600 kg m^{-3} d^{-1}.[5,32–35] To ensure that the simple NG method does not compromise one of CALF-20's key features, its water stability, the mec CALF-20 sample was soaked in water for 12 hours and analyzed by PXRD (Fig. S8). The results showed that the characteristic diffraction peaks remained unchanged, confirming that the crystalline structure was preserved after water exposure.

CO_2 adsorption measurements were conducted at 298 K to evaluate the performance of both mechanochemically and conventionally synthesized CALF-20 samples. Prior to testing, all samples were activated at 180 °C for 3 hours without any additional purification steps. As shown in Fig. 3b, the CO_2 adsorption capacity of mec CALF-20 with a grinding time of 15 minutes reached 3.57 mmol g^{-1} at 298 K and 1 bar, which is consistent with the values reported by Raganati *et al.* for CALF-20 synthesized *via* a LAG method.[28] To assess the

impact of purification on adsorption performance, the CO_2 uptake of the 15-minute ground mec CALF-20 sample was measured both with and without washing using deionized water (Fig. S9). The results showed negligible difference between the two, indicating that the washing is unnecessary in the present case since residual acetic acid can be simultaneously removed during the activation step. This result highlights a major advantage of the NG route, as it eliminates the needs for post-synthetic purification steps. By avoiding washing, the NG method simplifies the overall process, reduces solvent use and waste, and enhances scalability. Furthermore, the 45-minute ground mec CALF-20 sample demonstrated a CO_2 uptake comparable to that of the 15-minute ground sample, suggesting that extending the grinding time does not enhance gas adsorption performance. However, from a process efficiency standpoint, the 15-minute mec CALF-20 sample offers the highest STY, making it the most favorable condition for scalable production.

CALF-20 was also successfully synthesized on a gram scale through solvent-free mechanochemical synthesis using ball milling, with the reagent quantities scaled up by a factor of 10. The gram-scaled mec CALF-20 sample exhibits an average particle size of around 70.61 ± 23.03 nm and a phase similar to those observed in CALF-20 prepared *via* manual grinding (Fig. 4a and b). The CO_2 adsorption capacity also remains comparable, reaching up to 3.39 mmol g^{-1} at 298 K and 1 bar, as shown in Fig. 4c. Importantly, this synthesis delivered a high product yield of 97% along with an outstanding STY of 88 000 kg m^{-3} d^{-1}. These results demonstrate the reproducibility and scalability of the mechanochemical synthesis approach. Given its success at the gram scale, further scale-up using a screw extruder reactor is feasible. This reactor design offers several advantages, including continuous operation, enhanced mixing, precise control over reaction parameters, and suitability for industrial-scale production.[36,37] These features support the potential of dry mechanochemical synthesis as a practical and scalable route for CALF-20 manufacturing.

N_2 sorption isotherms of all samples were obtained at 77 K to investigate the textural properties of the CALF-20 samples. The conv CALF-20 sample exhibits a type I adsorption isotherm, typical of microporous materials (Fig. S10). The Brunauer–Emmett–Teller (BET) surface area and

total pore volume of conv CALF-20 were determined to be 551.24 m^2 g^{-1} and 0.2515 cm^3 g^{-1}, respectively. In contrast, both the mec CALF-20 and the gram-scaled mec CALF-20 demonstrate a type IV adsorption isotherm, indicating the presence of mesopores formed by interparticle voids. The BET surface area and total pore volume of the mec CALF-20 are 452.09 m^2 g^{-1} and 0.2282 cm^3 g^{-1}, respectively, while the gram-scale mec CALF-20 exhibited slightly higher values of 467.85 m^2 g^{-1} and 0.2692 cm^3 g^{-1}. These results highlight a key trade-off: while mechanochemical synthesis offers greater simplicity, scalability, and reduced solvent use, it can come at the cost of lower surface area and altered pore structure, which could impact performance in applications such as gas adsorption.

The solvent-free mechanochemical method not only achieves CO_2 adsorption performance comparable to that of conventional solvothermal synthesis but also offers several key advantages: (1) higher product yield and STY, (2) elimination of solvents and associated waste, (3) avoidance of high temperatures and long reaction times, and (4) simplified one-step synthesis without post-synthetic purification. As summarized in Table S1, this neat grinding approach achieves a η of zero and significantly enhances STY, highlighting its potential as a green and scalable alternative.

In terms of economic feasibility, this approach is substantially more cost-effective, reducing material costs by up to 10 times compared to the conventional route. As illustrated in Fig. S11, the primary cost component in CALF-20 synthesis is the zinc metal source, followed by the organic ligands and the solvent used during synthesis. By replacing the expensive zinc oxalate with zinc acetate, the major cost of the precursors can be substantially reduced. Although oxalic acid is still required, the absence of methanol minimizes the impact of ligand costs on total production expenses. The cost estimation is based on the laboratory-scale reagent prices, mostly sourced from Sigma-Aldrich. In addition, transitioning from conventional solvothermal synthesis to solvent-free mechanochemical grinding simplifies the overall process by eliminating filtration, washing, and drying steps, thereby reducing operational complexity and costs. This approach not only minimizes solvent use and environmental impact but also shortens reaction and post-processing times.
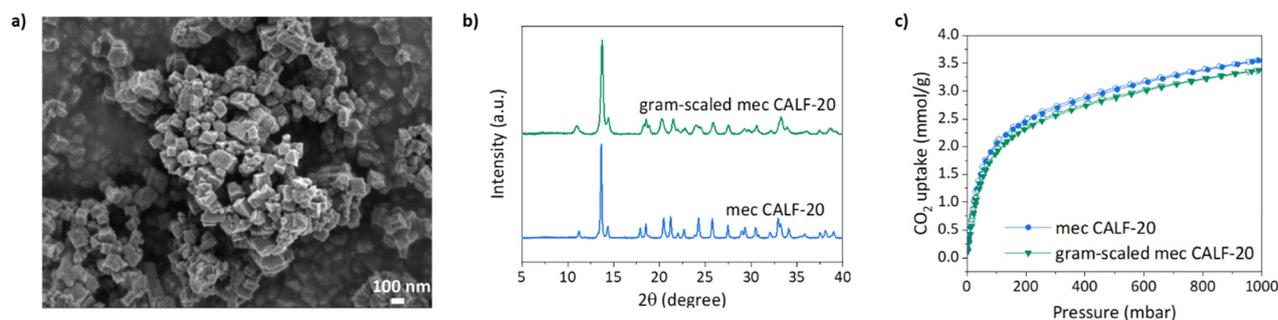

Fig. 4 (a) SEM image, (b) PXRD patterns, and (c) CO_2 adsorption isotherms of gram-scaled mec CALF-20 compared with mec CALF-20 at 298 K.

Its straightforward scalability makes it highly suitable for industrial implementation.

Conclusions

In summary, CALF-20 was successfully synthesized for the first time *via* a solvent-free mechanochemical route using stoichiometric precursors. This rapid, one-step process requires no purification and delivers a high yield of 97% (based on zinc) with a superior space–time yield of 88 000 kg m^{-3} d^{-1}, far exceeding the 550 kg m^{-3} d^{-1} of the optimized solvothermal method used at the commercial scale. The mechano-synthesized CALF-20 exhibits a CO_2 uptake comparable to the benchmark CALF-20, achieving 3.57 mmol g^{-1} at 298 K and 1 bar. Further studies are needed to scale up the synthesis beyond the gram scale and to evaluate its performance under realistic operating conditions.

Author contributions

N. P. and C. C. contributed equally. N. P., C. C.: investigation, methodology, and conceptualization; T. K. S., N. W., S. B.: supervision; T. K. S., S. B.: conceptualization; N. P., C. C., T. K. S., S. B.: writing – original draft, writing – review & editing.

Conflicts of interest

There are no conflicts to declare.

Data availability

Acknowledgements

Notes and references

1 J. Serafin, B. Dziejarski, O. F. Cruz Junior and J. Sreńscek-Nazzal, *Carbon*, 2023, **201**, 633–647.
2 C. Kim, S. N. Talapaneni and L. Dai, *Mater. Rep.: Energy*, 2023, **3**, 100199.
3 D. G. Boer, J. Langerak and P. P. Pescarmona, *ACS Appl. Energy Mater.*, 2023, **6**, 2634–2656.
4 S. Mahajan and M. Lahtinen, *J. Environ. Chem. Eng.*, 2022, **10**, 108930.
5 J. Pallarés, A. González-Cencerrado and I. Arauzo, *Biomass Bioenergy*, 2018, **115**, 64–73.
6 J. B. Lin, T. T. T. Nguyen, R. Vaidhyanathan, J. Burner, J. M. Taylor, H. Durekova, F. Akhtar, R. K. Mah, O. Ghaffari-Nik, S. Marx, N. Fylstra, S. S. Iremonger, K. W. Dawson, P. Sarkar, P. Hovington, A. Rajendran, T. K. Woo and G. K. H. Shimizu, *Science*, 2021, **374**, 1464–1469.
7 H. F. Hasan, F. T. Al-Sudani, T. M. Albayati, I. K. Salih, H. N. Hharah, H. S. Majdi, N. M. Cata Saady, S. Zendehboudi, A. Amari and S. A. Gheni, *Process Saf. Environ. Prot.*, 2024, **182**, 975–988.
8 F. Raganati and P. Ammendola, *Energy Fuels*, 2024, **38**, 13858–13905.
9 G. Ozin, *Adv. Sci. News*, 2022.
10 X. Wang, M. Alzayer, A. J. Shih, S. Bose, H. Xie, S. M. Vornholt, C. D. Malliakas, H. Alhashem, F. Joodaki, S. Marzouk, G. Xiong, M. Del Campo, P. Le Magueres, F. Formalik, D. Sengupta, K. B. Idrees, K. Ma, Y. Chen, K. O. Kirlikovali, T. Islamoglu, K. W. Chapman, R. Q. Snurr and O. K. Farha, *J. Am. Chem. Soc.*, 2024, **146**, 3943–3954.
11 R. Vaidhyanathan, S. S. Iremonger, K. W. Dawson and G. K. H. Shimizu, *Chem. Commun.*, 2009, 5230–5232.
12 Y. Higuchi, M. Sugita, S. Moriya, T. Takewaki and S. Tanaka, *Microporous Mesoporous Mater.*, 2024, **374**, 113137.
13 J.-L. Do and T. Friščić, *ACS Cent. Sci.*, 2017, **3**(1), 13–19.
14 M. Đud, O. Magdysyuk, D. Margetic and V. Štrukil, *Green Chem.*, 2016, **18**, 2666–2674.
15 J. L. Howard, W. Nicholson, Y. Sagatov and D. L. Browne, *Beilstein J. Org. Chem.*, 2017, **13**, 1950–1956.
16 L. E. Wenger and T. P. Hanusa, *Chem. Commun.*, 2023, **59**, 14210–14222.
17 M. Salari, M. Rezaee, S. P. H. Marashi and S. H. Aboutalebi, *Powder Technol.*, 2009, **192**, 54–57.
18 A. Ahmed, M. M. Islam, M. M. u. Islam, S. Masum, R. Islam and M. Molla, *Inorg. Nano-Met. Chem.*, 2020, **51**, 1–10.
19 T. Saothayanun and M. Ogawa, *Chem. Commun.*, 2021, **57**, 10003–10006.
20 A. Škrjanc, A. Golobič, M. Mazaj, M. Huš, B. Likozar and N. Z. Logar, *Microporous Mesoporous Mater.*, 2025, **384**, 113453.
21 P. J. Beldon, L. Fábián, R. S. Stein, A. Thirumurugan, A. K. Cheetham and T. Friščić, *Angew. Chem., Int. Ed.*, 2010, **49**, 9640–9643.
22 J. Beamish-Cook, K. Shankland, C. A. Murray and P. Vaqueiro, *Cryst. Growth Des.*, 2021, **21**, 3047–3055.
23 L. Ye, Y. Zhang, S. Jin, C. Zhou, J. Pang, Y. Luo, Y. Yu and W. Xu, *Inorg. Chem.*, 2024, **63**(43), 20572–20583.
24 M. Pilloni, F. Padella, G. Ennas, S. Lai, M. Bellusci, E. Rombi, F. Sini, M. Pentimalli, C. Delitala, A. Scano, V. Cabras and I. Ferino, *Microporous Mesoporous Mater.*, 2015, **213**, 14–21.
25 S. R. Wenger, E. R. Kearns, K. L. Miller and D. M. D'Alessandro, *ACS Appl. Energy Mater.*, 2023, **6**, 9074–9083.
26 M. Klimakow, P. Klobes, A. Thünemann, K. Rademann and F. Emmerling, *Chem. Mater.*, 2010, **22**, 5216–5221.
27 D. Prochowicz, K. Sokołowski, I. Justyniak, A. Kornowicz, D. Fairen-Jimenez, T. Friščić and J. Lewiński, *Chem. Commun.*, 2015, **51**, 4032–4035.
28 F. Raganati, M. Bellusci, F. Leardi, F. Varsano and P. Ammendola, *Chem. Eng. J.*, 2025, **506**, 159966.

29 Y. Wei, F. Qi, Y. Li, X. Min, Q. Wang, J. Hu and T. Sun, *RSC Adv.*, 2022, **12**, 18224–18231.

30 J. Drwęska, F. Formalik, K. Roztocki, R. Snurr, L. Barbour and A. Janiak, *Inorg. Chem.*, 2024, **63**(41), 19277–19286.

31 F. Raganati, F. Miccio and P. Ammendola, *Energy Fuels*, 2021, **35**, 12845–12868.

32 A. M. Wright, M. T. Kapelewski, S. Marx, O. K. Farha and W. Morris, *Nat. Mater.*, 2025, **24**, 178–187.

33 Z. Zheng, H. L. Nguyen, N. Hanikel, K. K.-Y. Li, Z. Zhou, T. Ma and O. M. Yaghi, *Nat. Protoc.*, 2023, **18**, 136–156.

34 M. I. Severino, E. Gkaniatsou, F. Nouar, M. L. Pinto and C. Serre, *Faraday Discuss.*, 2021, **231**, 326–341.

35 M. Gaab, N. Trukhan, S. Maurer, R. Gummaraju and U. Müller, *Microporous Mesoporous Mater.*, 2012, **157**, 131–136.

36 D. Crawford, J. Casaban, R. Haydon, N. Giri, T. McNally and S. L. James, *Chem. Sci.*, 2015, **6**, 1645–1649.

37 Y. Quan, R. Shen, R. Ma, Z. Zhang and Q. Wang, *ACS Sustainable Chem. Eng.*, 2022, **10**, 7216–7222.